A Machine Learning-based Solution for Monitoring of Converters in Smart Grid Application

Umaiz Sadiq[1], Fatma Mallek[2], Saif Ur Rehman[3], Rao Muhammad Asif[4], Ateeq Ur Rehman[*5], Habib Hamam[6]
Department of Electrical Engineering, The Superior University Lahore, Lahore, Pakistan[1,3,4]
Faculty of Engineering, Uni de Moncton, Moncton, NB E1A3E9, Canada[2,6]
School of Computing, Gachon University, Seongnam 13120, Republic of Korea[5]
Hodmas University College, Taleh Area, Mogadishu, Somalia[6]
Bridges for Academic Excellence, Tunis, Centre-Ville, Tunisia[6]
School of Electrical Engineering, University of Johannesburg, South Africa[6]

***Abstract*—The integration of renewable energy sources and the advancement of smart grid technologies have revolutionized the power distribution landscape. As the smart grid evolves, the monitoring and control of power converters play a crucial role in ensuring the stability and efficiency of the overall system. This research paper introduced a converter monitoring system in photovoltaic systems, the main concern is to protect the electrical system from disastrous failures that occur when the system is in operating condition. The reliability of the converters is significantly influenced by the degradation of their passive components, which can be characterized in various ways. For instance, the aging of inductors and capacitors can be characterized by a decrease in their inductance and capacitance values. Identifying which component is undergoing degradation and assessing whether it is in a critical condition or not, is crucial for implementing cost-effective maintenance strategies. This paper explores a set of classification algorithms, leveraging machine learning, trained on data collected from a Zeta converter simulated in Matlab Simulink. the report presents observations on how each algorithm effectively predicts the component and its condition and Graphical Performance Comparison for different ML Techniques serves as a crucial endeavor in evaluating and understanding the effectiveness of various ML approaches. The goal is to provide a comprehensive overview of how these techniques fare concerning criteria such as accuracy, precision, recall, F1 score, and Specificity among others. Quadratic Support Vector Machine (SVM) yields superior results compared to other machine learning techniques employed in training our dataset.**

***Keywords*—Artificial intelligence; photovoltaic; support vector machine; machine learning; K-Nearest neighbor; maximum power point tracking; pulse width modulation; prognostic analysis; one-against-rest; one-against-one; direct acyclic graph; multi class support vector machine; DC-DC converter; zeta c**

I. Introduction

The ever-expanding landscape of modern energy systems demands intelligent and adaptive technologies to manage the integration of renewable energy sources into power grids effectively. Smart grids have emerged as the linchpin in this transformative journey, offering enhanced control, resilience, and efficiency. At the heart of smart grid functionality lies the intricate interplay of power converters, such as inverters and rectifiers, which serve as the conduits for seamless energy flow, storage, and distribution [1]. The increased complexity and dynamism of contemporary smart grids necessitate advanced monitoring solutions for power converters. Traditional monitoring methods often struggle to keep pace with the rapid changes and diverse operational challenges posed by the integration of renewable energy [2]. This research endeavors to bridge this gap by introducing a novel machine-learning-based framework expressly designed for the real-time monitoring of converters within smart grid applications. The smart grid represents a paradigm shift in energy management, leveraging cutting-edge technologies to enhance grid flexibility, reliability, and sustainability. As renewable energy sources become integral to the energy matrix, the role of power converters in facilitating the seamless integration of solar, wind, and other green energy forms becomes paramount. Effective monitoring of these converters emerges as a critical component in ensuring the smooth operation of smart grids and harnessing the full potential of renewable resources. Against this backdrop, the primary objectives of this research are twofold. First, we aim to introduce a machine learning-based solution that significantly augments the real-time monitoring capabilities of power converters in smart grid applications. Second, we strive to enhance fault detection mechanisms, enabling the early identification of potential issues within the converter systems. Additionally, the research seeks to optimize maintenance strategies, providing a proactive approach to addressing challenges and ensuring the longevity and resilience of smart grid infrastructures [3]. By leveraging the capabilities of machine learning algorithms, this study aims to unravel intricate patterns within the operational data of power converters, facilitating timely interventions, and ultimately contributing to the overall stability and efficiency of smart grid systems [4]. The proposed solution aligns with the overarching goal of advancing smart grids into adaptive, self-regulating entities capable of seamlessly accommodating the evolving landscape of renewable energy integration.

A. Literature Review

Predictive maintenance is becoming increasingly important for power electronic converters. In [5] proposes a circuit-based approach. It utilizes a combination of filters and a Relevance Vector Machine (RVM) algorithm to analyze the output voltage response of the converter. The cosine distance between the measured response and a reference is fed to the RVM, which then estimates the remaining useful life (RUL) of the entire circuit. In [6] focuses on individual component health. It uses a Buck converter as a test case. By monitoring various electrical parameters (inductor current, capacitor voltage/current, output voltage, and their ripple) under controlled

component degradation, the authors train an Artificial Neural Network (ANN) to estimate the current parameter value of a degrading component (e.g., inductor or capacitor). This allows preventative maintenance before the component reaches critical failure. The ANN is also used for fault diagnostics. In [7] explores fault identification using a simulated three-parallel power conversion system for a wind turbine. By analyzing the dq-transformed three-phase measured currents, a neural network is trained to identify faulty switches based on characteristic current patterns that emerge in the dq-frame when a switch malfunctions. In [8] focuses on anomaly detection. The authors vary component values (capacitor and inductor) in a super-buck converter and collect statistical features (mean and standard deviation) of the output voltage. By calculating the Mahalanobis distance between these features and a baseline, they can detect deviations caused by component degradation. This information is then used to train a Machine Learning (ML) algorithm for RUL prediction of the entire converter. In [9] proposes a method to identify problems in power converters early, especially for modular multilevel converters (MMCs). Method involves training a special type of artificial intelligence (AI) called a one-class classifier. This AI learns what normal operation looks like and can then flag any unexpected changes, even if it hasn't been specifically trained to recognize every possible problem. In [10] focuses on finding problems within the system that converts electricity into motion (electromechanical conversion chain) in both regular and self-driving electric vehicles (EVs). Electric vehicles have many sensors that track things like electricity flow (current), voltage, and motor speed. This information is used to identify any issues within the system. This study offers a new way to diagnose faults by using a special technique called "feature extraction" which helps identify important patterns in the data. The specific approach proposed here is called Long Short-Term Memory (LSTM), a type of artificial intelligence well-suited for analyzing sequences of data like sensor readings. In [11] introduces a method for estimating important properties (parameters) in electronic circuits (power converters) that combines machine learning with the known physics of how the circuits work (Physics-informed machine learning, PIML). This method is demonstrated using a common circuit called a dc-dc Buck converter. Combine deep neural network with the existing knowledge about how the circuit behaves. In [12] examines how reliable boost converters (a type of electrical circuit) with feedback control are over time. The research shows that these converters become less reliable as they age. The paper introduces a method to calculate this decreasing reliability, considering how different parts of the circuit wear out and change over time. In [13] proposes a method to predict how well DC-DC power converters will function over time (prognosis). First, the authors review existing methods for predicting converter health. They then focus on how capacitors degrade over time, considering both the heating caused by small current fluctuations (ripple current) and the underlying physics of how heat damages capacitors. This information about capacitor degradation is then fed back into the overall model of the DC-DC converter to see how its performance changes. The researchers use computer simulations (Monte Carlo methods) to explore this under various conditions. Finally, they discuss the results of these simulations and how real-world experiments can be used to verify the accuracy of their model.

B. Contribution

Unlike previous research, in this paper, the establishment and validation of a monitoring system designed for identifying faults in DC-DC converters involve defining its operational parameters. This process is meticulously executed and subsequently verified through a comprehensive simulation procedure conducted within the Matlab-Simulink environment [14]. The converter under scrutiny in this investigation is specifically a Zeta converter, chosen for its unique capabilities in achieving a substantial voltage gain and minimizing output current ripple. This advantageous feature is made possible through the strategic utilization of four passive components. This paper focuses on the specialized domain of prognostics, honing in on the prognostic challenges presented by a DC-DC converter integrated with a photovoltaic (PV) input [15]-[16]. This particular scenario introduces two distinct challenges that complicate the prognostic analysis. The first challenge stems from the non-linear current-voltage characteristics of the PV source, leading to non-conforming trends in converter current and voltages when compared to the more predictable ideal voltage and current sources commonly employed in diagnostic and prognostic scenarios. The second challenge involves the intricate functional relationship between these characteristics and environmental factors such as temperature and irradiance. This dynamic interplay introduces complexities that have the potential to result in inaccurate classifications of the converter's operational state. To tackle this inherent problem, a specialized normalization approach is employed. This approach serves the crucial purpose of untangling the prognostic-sensitive quantities from the environment-dependent nature of the PV source. By doing so, it aims to mitigate potential errors in the prognostic classification of the converter's working condition, ensuring a more accurate and robust analysis in the presence of non-linear Photovoltaic characteristics and environmental variables [17]. Subsequently, we subject the system to three distinct operating conditions to meticulously record readings about the current and voltages across the passive elements of the converter, relative to their inductance and capacitance values [18]. This process is crucial in establishing a comprehensive dataset that serves as the foundation for subsequent training endeavors. Following the data collection phase, we employ various machine learning techniques to process and train the acquired dataset. Our objective is to evaluate the performance of these techniques and discern the most effective approach in terms of classification accuracy. The ensuing comparative analysis sheds light on the strengths and weaknesses of each method, facilitating the identification of the most promising technique for robust classification results. Through this methodical exploration, our research contributes valuable insights to the selection of the optimal machine-learning technique for converter monitoring [19]. The identification of a superior technique holds significant implications for enhancing the accuracy and reliability of monitoring systems in photovoltaic applications within smart grid environments. The main elements of originality may be summarized as follows:

- Development and Validation of a Machine Learning-Based Monitoring System: The paper introduces a novel machine learning-based system specifically tailored for monitoring zeta converters in pv systems [20]. This system's ability to accurately predict the

condition of components and distinguish between nominal and malfunctioning states underpins its original contribution to the field of smart grid technology.

- Comprehensive evaluation of multiple machine learning techniques for fault detection: A significant contribution of the research is the thorough comparison and evaluation of various machine learning techniques, including Support Vector Machine (SVM) with different kernels, K-Nearest Neighbors (KNN) with various distance metrics, and Decision Trees with different complexities. This comprehensive analysis offers valuable insights into the most effective methods for fault detection in Zeta converters, highlighting the superiority of the linear SVM approach [21].
- Optimization of multi-class SVM for predictive maintenance: The paper showcases the optimization of a multi-class SVM classifier, demonstrating its outstanding performance in predicting component conditions across a wide range of operational scenarios. This includes the algorithm's robustness in identifying specific components undergoing degradation, marking a notable advancement in the predictive maintenance of photovoltaic systems.
- In-depth analysis of renewable energy variations on zeta Converter performance: The research provides a detailed investigation into how fluctuations in renewable energy sources impact the operational stability and efficiency of zeta converters. By simulating various renewable energy conditions and analyzing their effects on the converter's passive components, the study contributes novel insights into optimizing photovoltaic systems for improved performance [22].
- Practical implications for real-time monitoring and preventive maintenance: The study's findings have significant practical implications for the real-time monitoring and preventive maintenance of zeta converters within smart grid applications. By leveraging the developed machine learning-based monitoring system, the paper offers a scalable solution for enhancing the reliability and sustainability of systems integrated with renewable energy sources, addressing a critical need in the evolving landscape of smart [23].

In the subsequent sections, we delve into an extensive review of existing literature, outline our robust methodology, present empirical results, and discuss the broader implications and future directions of this machine learning-based approach to converter monitoring in smart grid applications. Through this exploration, we seek to fortify the foundations of smart grid technologies and propel the transition toward a more sustainable and resilient energy future [24].

II. Photovoltaic System Design Procedure

The proposed analytical approach is centered around a photovoltaic system comprising a 230 W solar panel integrated with a zeta converter, connected to a 48 V DC microgrid. The primary function of the DC-DC converter is to facilitate efficient energy transfer from the solar source to the grid. Multiple techniques, such as Maximum Power Point Tracking (MPPT) control [25], can be employed to optimize this energy transfer process. The MPPT algorithm, specifically tasked with controlling the converter duty cycle (D), is instrumental in attaining an optimal operating point on the photovoltaic source. While traditional MPPT algorithms often focus on setting the source voltage close to the maximum power voltage, the choice of a tracking algorithm or model-based algorithm, potentially leveraging machine learning methods, depends on the desired outcome. Notably, this paper does not simulate the MPPT algorithm as it is not a pivotal aspect of the prognostic analysis. The core concept of the monitoring procedure lies in maintaining a fixed duty cycle during the brief intervals necessary for extracting voltage and current measurements. This strategic approach avoids disrupting the converter's operation, allowing the definition of its state of health without interrupting energy transfer. During the prognostic analysis, the duty cycle remains constant, avoiding the pursuit of the maximum power point. This deliberate choice limits measurement variability, streamlining the identification of malfunctions. Post-prognosis, the MPPT algorithm can once again adjust the duty cycle. Importantly, the measurement procedure's minimal impact on energy production, requiring only a few periods at the converter switching frequency, ensures that the prognostic analysis does not significantly interfere with the overall energy generation process [25].

A. Renewable Energy Source

The energy source under examination within this study is a solar panel with a power rating of 230 W, incorporating a configuration of 60 multicrystalline cells identified as TW230P60-FA, courtesy of Tianwei New Energy. Crucial electrical parameters characterizing the panel are derived from its datasheet and comprehensively outlined in Table I. In this table, VMPP and IMPP represent the maximum power point voltage and current, respectively, while VOC signifies the open-circuit voltage, and ISC denotes the short-circuit current. These fundamental specifications serve as the foundation for understanding and analyzing the solar panel's performance characteristics in the subsequent phases of the research [25]. Leveraging these inherent characteristics, the implementation of an equivalent circuit model within the Simulink environment for the solar panel becomes feasible. This model allows for the extraction of voltage–current curves, offering a dynamic representation of how these curves respond to variations in solar irradiance and operational temperature. Undoubtedly, the input current and voltage of the DC-DC converter are intricately linked to prevailing environmental conditions, manifesting in the internal electrical characteristics of the converter. As the measurements derived from the converter serve as critical indicators for assessing its state of health, their sensitivity to fluctuations in input current and voltage extends to the environmental conditions of the PV device. This dual sensitivity poses a challenge during the classification of malfunctions, demanding the monitoring system's capability to distinguish variations induced by component aging from those arising due to alterations in solar irradiance and operational temperature. To address this potential confusion, a straightforward approach could involve incorporating irradiance and temperature values into the set of measurements processed by the classifier. However, the practical feasibility of measuring these quantities is often challenging, and such an approach significantly

TABLE I. CHARACTERISTICS OF THE PHOTOVOLTAIC PANEL

Vmpp	Impp	Voc	Isc	Ncell
29.4V	7.82A	37.3V	8.22A	60

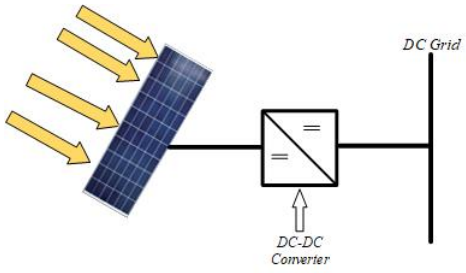

Fig. 1. Photovoltic system with DC-DC converter.

complicates the training stage by necessitating an extensive dataset. In this paper, a novel graphical method is proposed to circumvent these challenges, aiming to select time-domain measurements that exhibit lower sensitivity to variations in solar irradiance and temperature.

B. Zeta Converter

A zeta converter is a type of DC-DC power converter that operates with a unique topology, making it particularly suitable for applications like PV systems. The zeta converter combines the features of a buck and a boost converter, providing advantages such as a high voltage gain and reduced output current ripple [25]. zeta converter is a non-isolated converter topology that combines the buck-boost and buck converters. It allows both step-up and step-down voltage conversion. The basic components of a zeta converter include an inductor (L), a capacitor (C), a diode (D), and a switch (S). The key advantage of the zeta converter is its ability to achieve a high voltage gain. This is particularly beneficial in photovoltaic systems where maximizing the voltage output is crucial for efficient energy harvesting. In a photovoltaic system, the zeta converter is often employed to interface the solar panel with the power grid or energy storage system Fig. 1. The zeta converter can operate with a variable input voltage from the solar panel, accommodating fluctuations in solar irradiance [25]. The zeta converter facilitates energy transfer from the photovoltaic source to the load or grid by efficiently adjusting the duty cycle of the switching operation. It ensures optimal power transfer by dynamically adapting to changes in solar irradiance and operating conditions. The entire system, as depicted in Fig. 2 and employed throughout the simulation process in Simulink, showcases the implementation of a Pulse Width Modulation (PWM) technique to drive the converter switches S1 and S2. These switches, consisting of N-channel Power MOSFETs, operate in opposite phases. During the conduction mode of switch S1, the inductor L1 absorbs energy from the DC source, while concurrently, L2 absorbs energy from both the source and capacitor C1. This dynamic results in the input current, iS(t), being the sum of iL1(t) and iL2(t). Conversely, in the opposite condition (S1 Off and S2 On), the input current becomes zero, and the current iL1(t) flows through S2 to charge capacitor C1. Simultaneously, iL2(t)

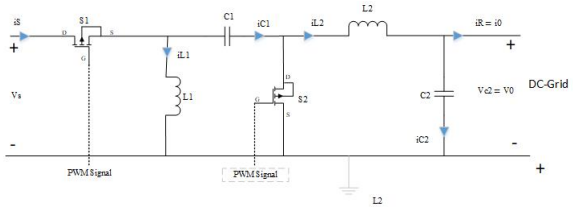

Fig. 2. Circuit diagram of the zeta converter.

traverses the circuit (C2-R) and returns through the closed switch S2. This alternating operation of the switches, in tandem with the energy absorption and flow through the inductors and capacitors, forms the operational essence of the zeta converter in the photovoltaic system. The intricacies of these current and voltage dynamics, influenced by varying solar irradiance and temperature conditions, are effectively captured and analyzed within the Simulink model, contributing to a comprehensive understanding of the system's behavior. The currents iL1(t) , iL2(t), and iS2(t) exhibit distinct ripples, denoted as ΔiL1(t), ΔiL2(t), and ΔiS2(t), respectively. Among these, ΔiS2(t) holds particular significance as it determines the conduction mode of the circuit. If the current iS2(t) reaches zero during the switch-Off period, the converter operates in the Discontinuous Conduction Mode (DCM). Conversely, if iS2(t) maintains a non-zero value during the switch transition from off to on, the Continuous Conduction Mode (CCM) is established. Opting for CCM proves advantageous as it allows for a reduction in electrical stress on the converter components and results in a diminished ripple on the output quantities. Therefore, this work exclusively considers the CCM, and the analog components are dimensioned accordingly to ensure this operational condition. This deliberate choice aligns intending to achieve optimal performance and reliability in the zeta converter, emphasizing the importance of meticulous component sizing to maintain continuous conduction and mitigate potential issues associated with discontinuous operation [25].

C. Mathematical Modeling

Modeling a zeta converter mathematically involves creating a set of equations that describe its behavior. A zeta Converter is a type of DC-DC converter that combines the features of a buck-boost converter and a sepic converter. Here, a simplified mathematical model is being provided of a zeta Converter [26]. The zeta Converter circuit consists of an input inductor (L1), an input capacitor (C1), a switch (S), a diode (D), an output inductor (L2), an output capacitor (C2), and a load resistor (R).

D. Voltage Relations

Input Voltage (Vin) and Output Voltage (Vout)

$$Vin = L1.\frac{diL1}{dt} + Vc1 = L2.\frac{diL2}{dt} + Vc2 + Vout \quad (1)$$

where VC1 and VC2 are the voltages across capacitors C1 and C2, respectively.

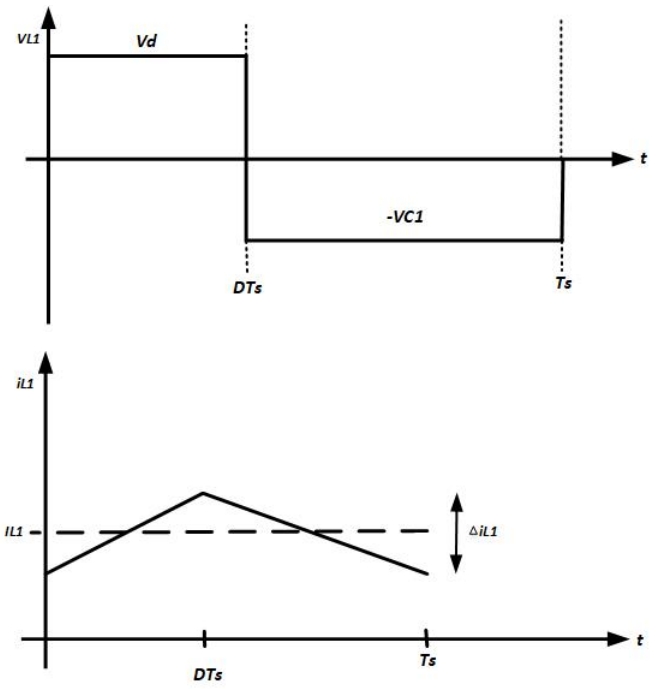

Fig. 3. Voltage and current waveforms of inductor L1 [26].

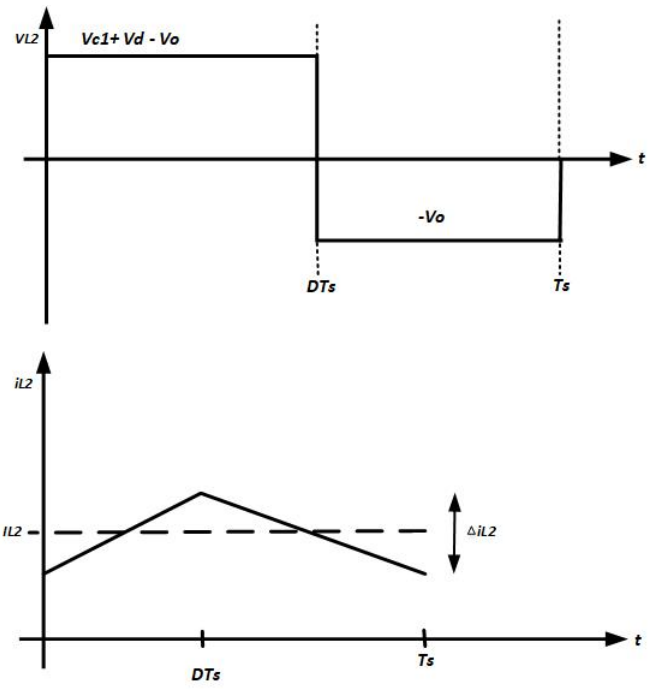

Fig. 4. Voltage and current waveforms of inductor L2 [26].

E. Current Relations

Current through the input inductor iL1

$$Vin = L1.\frac{diL1}{dt} + Vc1 \tag{2}$$

$$Vin = L2.\frac{diL2}{dt} + Vc2 \tag{3}$$

Current through the output inductor iL2

$$Vc2 = L2\frac{diL2}{dt} + Vout \tag{4}$$

Current through the diode iD

$$ID = IL1 - IL2 \tag{5}$$

F. Derivation of the Zeta Converter

In the following section, we use lowercase letters 'v' and 'i' to denote instantaneous values of voltages and currents, respectively. Meanwhile, uppercase letters 'V' and 'I' are utilized to represent average voltage and currents. The switch commences operation at t = 0 and stays active until t = DTs, where Ts represents the switching period, and D corresponds to the duty cycle [26]. The voltage and current waveforms of inductor L1 are depicted in Fig. 3. In the context of the converter functioning in a steady state and CCM, we assume that the inductor's current commences and concludes a full switching period at the same level. This condition is often referred to as the volt-second balance, signifying that the average applied voltage across the inductor amounts to zero during a single switching period, as expressed by the equation.

$$\frac{1}{Ts}\int_0^{Ts} VL1dt = 0 \tag{6}$$

Dividing the complete switching period, Ts, into two intervals during which the switch is activated and deactivated.

$$\frac{1}{Ts}(\int_0^{DTs} VL1dt + \int_{DTs}^{Ts} VL1dt) = 0 \tag{7}$$

$$\frac{1}{Ts}(Vd.DTs - Vc1(1-D)Ts) = 0 \tag{8}$$

$$Vd.DTs - Vc1(1-D) = 0 \tag{9}$$

Rearranging to get an expression for VC1 equals

$$Vc1 = Vd.\frac{D}{1-D} \tag{10}$$

Likewise, Fig. 4 illustrates the voltage and current profiles of inductor L2. The determination of the volt-second balance for L2 is computed as follows:

$$\frac{1}{Ts}\int_0^{Ts} VL1dt = 0 \tag{11}$$

$$D(Vc1 + Vd - Vo) - Vo(1-D) = 0 \tag{12}$$

$$D.Vc1 + D.Vd - D.Vo - Vo + D.Vo = 0 \tag{13}$$

By collecting terms this equals

$$Vo = D.Vc1 + D.Vd \tag{14}$$

[**?**] Again, this is rearranged for VC1 to equal

$$Vd.\frac{D}{1-D} = \frac{Vo}{D} - Vd \tag{15}$$

By combining (1) and (2)

$$\frac{Vo}{D} = Vd.\frac{D}{1-D} + Vd \tag{16}$$

Expression is then solved for the conversion ratio, M = Vo

$$\frac{Vo}{D} = \frac{D^2 + D(1-D)}{1-D} \tag{17}$$

$$M = \frac{Vo}{Vd} = \frac{D}{1-D} \tag{18}$$

$$D = \frac{Vo}{Vd + Vo} \tag{19}$$

by combining all terms

$$Vd = Vo.\frac{1-D}{D} \tag{20}$$

Alternatively, it may be solved for the duty cycle

$$Vc1 = Vd.\frac{D}{1-D} = Vo.\frac{1-D}{D}\frac{D}{1-D} \tag{21}$$

$$Vc1 = Vo \tag{22}$$

During steady-state operation, the volt-second balance implies that the average voltage across the inductors is zero. Consequently, in steady-state operation, applying Kirchhoff's voltage law to the loop involving L1, C1, L2, and the output Vo indicates that the average voltage across the capacitor must be equal to the output Vo. Under the steady-state assumption that the output capacitor Co is adequately sized to maintain a stable voltage, we can also infer that.

$$Vc2 = Vo \tag{23}$$

As we analyze the information provided in the diagram, it becomes apparent that, during steady-state conditions, the average current in the capacitors is zero. Consequently, by applying Kirchhoff's current law, we derive the following:

$$IL1 = Id \tag{24}$$

and

$$IL2 = Io \tag{25}$$

G. Fault Classes

In proposing a prognostic approach for photovoltaic systems, specifically targeting parametric faults, it is essential to establish corresponding classes by defining tolerance ranges around the nominal values of system components. Parametric faults involve deviations of components from their nominal values, leading to a partial loss of functionality. While these deviations may initially have subtle effects on the system's performance, selecting appropriate measurements enables the identification and localization of variations in specific components or groups of components. Table II summarizes the operating ranges for each component with a 15 percent tolerance applied. These variations are deemed acceptable as they ensure an output ripple of less than 10 percent and maintain CCM operation. Parametric failure conditions are defined as a maximum decrease of 70 percent for each passive component [27]. It is crucial to underscore the adoption of the single failure hypothesis due to its high probability, and there is an expectation of no fault propagation. This means that only one passive component at a time is assumed to be faulty, leading to the identification of five classes of failure. The nominal operating condition of the converter is denoted as "class 0", where all components remain within their nominal ranges. The additional classes are detailed in Table III.

TABLE II. PASSIVE ELEMENTS OPERATING RANGES

	L1 (mH)	L2 (mH)	C1 (uF)	C2 (uF)
Nominal Range	(4.25-5.75)	(4.25-5.75)	(2.04-2.76)	(2.04-2.76)
Malfunction Condition	(1.5-4.25)	(1.5-4.25)	(0.72-2.04)	(0.72-2.04)

TABLE III. DEFINING FAULTS CLASSES

Fault Class	Description
FC0	All components in nominal range
FC1	Fault occur in inductor L1
FC2	Fault occur in inductor L2
FC3	Fault occur in capacitor C1
FC4	Fault occur in capacitor C2

III. TRAINING DATASET FROM ZETA CONVERTER MODEL

Ensuring similarity between training and testing datasets that an SVM will classify during testing is crucial. The most effective way to acquire training datasets is by gathering patterns from the same sensors and circuits utilized for the testing datasets. However, applying a two-class SVM to a real-world circuit makes this impractical. This is due to the necessity for training datasets to encompass example patterns from each class intended for classification, often abundant for normal conditions but typically lacking for faulty conditions [28]. Two potential solutions are identified: first, physically altering the circuit, posing risks of permanent damage; second, simulating faulty conditions using a model. Given the unfeasibility of the first option, example patterns and training datasets will be derived using finite element converter models. Implementing converter models introduces a new layer of complexity to this paper. Decisions regarding model complexity, passive elements, and shell types become pivotal. These decisions hinge on simulating the complexity of the faults to be replicated. Upon making these decisions, validating and updating the model to align with the actual circuit is essential. A typical validation approach involves a modal comparison with the real circuit, along with passive elements tests. Challenges arise in extracting dynamic data from the model and applying appropriate excitation. Though an ideal approach involves random loadings similar to real-world environmental and operational conditions, statistical information on these loadings is challenging to obtain and computationally intensive to simulate. Instead, the chosen approach concentrates on utilizing impact loading. Characteristics of this impact include duration based on the circuit's frequency content, an arbitrary magnitude ensuring the circuit's response remains linear, and selecting a regularly excited point on the actual circuit as the location [30]. Following these considerations, a training dataset can be constructed according to Table IV.

TABLE IV. FEATURE CONSIDERED FOR TRAINING DATA SET

Temp	Irrad	VC1	VC2	IL1	IL2
20	600	-85.87	32.53	4.901	3.182

A. Generate Data under Various Operating Conditions

Conducted an in-depth analysis of the behavior of passive elements within the Zeta converter under varying temperature and irradiance conditions. The Zeta converter comprises four crucial passive components Capacitor C1, Capacitor C2, Inductor L1, and Inductor L2. Each of these components possesses specific specifications within nominal ranges, as well as malfunction ranges, which have been meticulously documented. Under different temperature and irradiance conditions, observed that the capacitance and inductance of these passive elements fluctuated over time. To capture this dynamic behavior, collected extensive data through a comprehensive procedure:

1) Initial data gathering 400 readings: Initiated the data collection process under specific conditions—temperature at 20 degrees Celsius and irradiance at 600 units. Recorded 400 data points for voltages across capacitors C1 and C2 and currents across inductors L1 and L2. As temperature and irradiance changed, the capacitance and inductance of these passive elements evolved, subsequently affecting the voltages and currents across them.

2) Data recording and structuring: To systematically record these changes, created an Excel spreadsheet. It featured ten columns: the first two columns maintained a constant temperature of 20 degrees and irradiance of 600 units, respectively. The subsequent columns captured varying parameters: capacitance of C1, inductance of L1, capacitance of C2, and inductance of L2. These parameters changed over time within the nominal ranges, which were defined for data collection. The final four columns represented voltage across C1, current across L1, voltage across C2, and current across L2, respectively.

3) Defining fault classes: To categorize the data appropriately, introduced four fault classes fault class 1 (FC1), fault class 2 (FC2), fault class 3 (FC3), and fault class 4 (FC4) based on specific conditions and readings. When the capacitance and inductance of passive elements fell within the nominal range, the data points belonged to the zero-fault class.

4) Subsequent data collection 100 readings: Following the initial phase, continued data collection with identical conditions but introduced variations. The capacitance and inductance ranges of passive elements shifted from nominal to malfunction ranges. Divided this phase into four segments:

- The first 25 readings involved altering the capacitance of C1 while maintaining the other three elements within their ideal specifications falling under fault class 1.
- The next 25 readings focused on changing the inductance of L1 while keeping the other elements unchanged falling under fault class 2.
- Similarly, the third set of 25 readings pertained to modifying the inductance of L2, while the other elements retained their original values falling under fault class 3.
- The final 25 readings centered on adjusting the capacitance of C2, with the other element values remaining unchanged falling under fault class 4.

5) Total data collection: In total, 500 readings under the same temperature of 20 degrees, and irradiance of 600 units.

6) Variation in conditions: To expand the dataset, altered the temperature to 70 degrees and irradiance to 1000 units, resulting in an additional 500 readings. Among these readings, 400 had all passive elements within their nominal ranges, classifying as the zero-fault class. The remaining 100 readings exhibited variations, with each passive element's capacitance or inductance changing while the others remained unaltered. These 100 readings were divided into four sets of 25 readings, each assigned a fault class.

7) Further temperature and irradiance variation: Repeated this procedure with a temperature of 80 degrees and irradiance at 1200 units, adding another 500 readings.

B. Data Splitting

After compiling the dataset, partitioned it into two sets: a training dataset comprising 70 percent of the data and a test dataset containing 30 percent of the data. This separation facilitated model training using the training dataset, followed by testing and evaluation using the test dataset.

IV. Sensitivity Analysis

In an electrical circuit, the values of its components will probably change over time. These modifications will affect the circuit's output response, particularly the output voltage, with other current and voltages throughout the circuit. Assess the magnitude of the impact of a specific parameter change on a particular voltage or current, Analysis becomes indispensable. Hence, Analysis is employed to scrutinize the consequences of a deviation in the value of one component from its standard state on a specific output of interest in a system. Sensitivity analysis is widely applicable in diverse fields such as ecology, chemistry, semiconductor materials, and economics, contributing to decision-making processes. In the realm of power converters, Analysis plays a pivotal role in optimizing the design of electrical circuits. However, in our context, By using sensitivity methods to know how specific features change their properties by changes in one of the parameter components properties within the zeta converter. This investigation is valuable for comprehending alterations in features (or inputs) when a component undergoes modification, thereby aiding in the generation of training data for machine learning applications [25]. Sensitivity analysis in microsoft excel involves assessing how changes in certain input variables (parameters) affect the output of a model or calculation. Here's a step-by-step guide on how to perform sensitivity analysis using Excel: Following these steps, you can conduct sensitivity analysis in Excel to assess the impact of varying input parameters on your model or calculations, helping you make informed decisions and understand the robustness of your models.

1) Set up Your excel spreadsheet:

- Open a new or existing excel spreadsheet.
- Organize the data including temperature, irradiance, capacitor 1 voltages (VC1), capacitor 2 voltages (VC2), inductor current (IL1), inductor 2 current (IL2). Collected the 1500 voltages and currents readings of passive components C1, C2, L1, and L2.

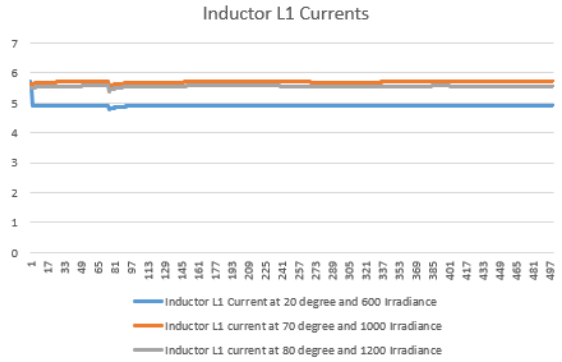

Fig. 5. IL1 variations.

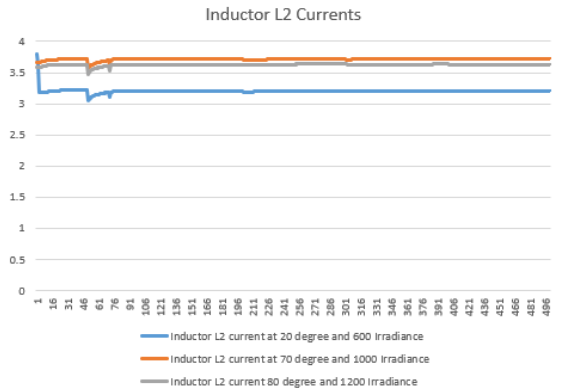

Fig. 6. IL2 variations.

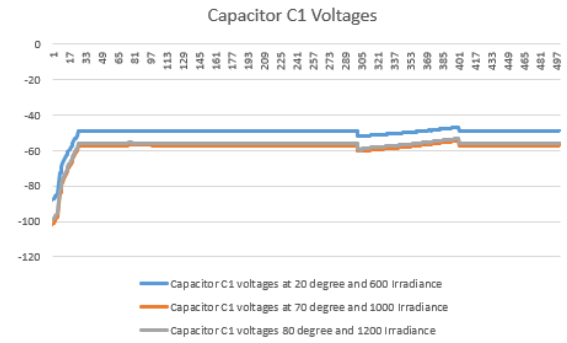

Fig. 7. VC1 variations.

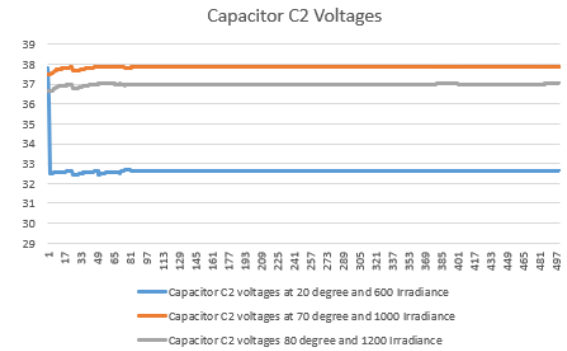

Fig. 8. VC2 variations.

A. Identify the Input and Output Cells

- Temperature, irradiance, IL1, VC1, VC2, and IL2 are the input parameters containing cells E1, F1, G1, H1, I1, and J1 these are the parameter which would have to vary for sensitivity analysis.
- E2, F2, G2, H2 cells that contain the formula or calculation whose results would be analyzed. H2 is the output cell that will display the impact of changing input values.

B. Analyze and Interpret the Results

After setting the Excel sheet data set which contained 3 different operating conditions which are given below:

- 20 degree temperature and 600 irradiance.
- 70 degree temperature and 1000 irradiance.
- 80 degree temperature and 1200 irradiance.

Collected 1500 current and voltage of passive elements readings, each operating condition contained 500 readings. After setting the data set now analyzed how each passive element's Voltages and Current changes for some readings and 3 operating conditions mentioned above: Fig. 5 and 6 depict graphs illustrating the variation of IL1 and IL2, respectively, across different operating conditions. Meanwhile, Fig. 7 and 8 display graphs representing the variation of VC1 and VC2, respectively, under various operating conditions. Graph IL1 and IL2 present current across inductors with 3 operating conditions changes for some readings

V. SVM Architecture

SVM is a supervised machine learning algorithm employed for classification and regression tasks, with notable popularity in solving classification problems [28]. SVM operates on the principle of identifying a hyperplane that effectively separates distinct classes of data points within a high-dimensional feature space. Below is a concise overview of the architecture and fundamental components of an SVM:

A. Input Data

The SVM algorithm is initiated by feeding it a meticulously labeled dataset, much like the dataset has been carefully assembled. This dataset comprises an array of distinctive features or attributes, each bearing significance in the analysis. These encompass temperature, irradiance, capacitance values for C1 and C2, inductance values for L1 and L2, as well as voltage and current measurements across C1, C2, L1, and L2. Alongside these feature attributes, the dataset also includes corresponding class labels, signifying specific fault conditions. It's noteworthy that SVM, renowned for its prowess in binary classification, is the chosen methodology for this particular dataset. This means that SVM is employed to categorize the data into one of two classes. The SVM algorithm will diligently scrutinize the interplay of these attributes and their relevance to the fault classes, effectively classifying the data points into the aforementioned fault categories. The goal is to distinguish between these classes with precision, leveraging the distinctiveness of the dataset's attributes.

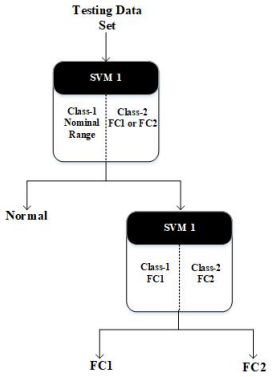

Fig. 9. Two class SVM network.

B. Multi-class Classification with SVM Networks

The term "two-class SVM" implies its restricted capacity to classify patterns into just two classes. This limitation poses a challenge for circuit fault detection due to the diverse range of potential fault conditions or classes that may occur in any given circuit. To address this issue, employing a network of two-class SVMs becomes a viable solution. Fig. 9 is the two-class SVM network that is capable of detecting the fault between two fault classes. From the depicted diagram, a testing dataset is input into SVM-1, which classifies it as originating from either a normal circuit condition or from a faulty circuit afflicted with FC1 or FC2. If the majority of the dataset is labeled as normal, the tree-like network concludes at that point. However, if the majority of the data is identified as a faulty condition, the dataset is directed to SVM-2, where it determines whether the structure is experiencing FC1 or FC2. Notably, this paper does not employ a specific routine to define an optimal network. Instead, these decisions are made based on considerations of the circuit and the specific faults targeted for detection [29]. Detection of the faults will be done using the tree-like SVM network shown in Fig. 10. A testing dataset is input to SVM-1 and classified as either class-1 which is normal operating mode, or class-2 which is any of the faults FC1-FC4. If the majority of data is classified as healthy the tree-like network ends. However, if the majority of data is classified as class-2 then more SVMs must be used to determine the location of the faults. Accordingly, data is input to SVM-2 which determines the capacitors that the fault is located on. And then, depending on the results from SVM-2, the data is input to either SVM-3 or SVM-4 to determine whether the fault is on inductors.

C. Types of Multi-class SVM

There are three types of multi-class SVM:

1) One-against-rest (OvR)
2) One-against-one (OvO)
3) Direct acyclic graph (DAG)

Used one-against-rest type to evaluate our results. its algorithms is given below:

1) One-against-rest: OvR also known as one-vs-all, is a strategy used in multiclass classification. In the case of SVM, it involves training multiple binary classifiers, where each class is treated as a binary classification problem against all other classes [29]. Let's denote the set of classes as

$$C = \{C1, C2, , , , , , Ck\} \tag{26}$$

where k represents the total number of classes. The mathematical equation for the one-against-rest multi-class SVM involves training *k* binary SVM classifiers, one for each class. For a class C*i* the classifier is trained to distinguish instances of C*i* from all the other classes collectively. The decision function for each class C*i* is:

$$Fi(x) = sign(Wi.x + bi) \tag{27}$$

$$Fi(x) = sign(Wi.x + bi) \tag{28}$$

Where:

1) *Fi*(x) represents the decision function for class C*i*.
2) *Wi* is the weight vector for class C*i*.
3) *x* represents the input feature vector.
4) *bi* is the bias term for class C*i*.

During training, the SVM is trained to learn the decision boundary that separates instances of the current class C *i* from all other classes (as a binary classification problem). This process is repeated for each class in the dataset, resulting in *k* separate binary classifiers, each handling the distinction of one class from the rest. At prediction time, the final class assignment for a new instance is determined by selecting the class associated with the classifier that yields the highest confidence or decision value [29]-[30]. This OvR approach allows the SVM to handle multi-class classification problems by breaking them down into a series of binary classification sub-problems, which are then collectively used to predict the final class for a given input.

VI. Evaluation Metrics

To ascertain the efficacy of these techniques and sub-techniques, several key evaluation metrics were calculated from the confusion matrices generated for each method. These metrics included:

A. Precision

Precision serves as a pivotal performance metric for assessing the accuracy of a classification model. It quantifies the ratio of accurately predicted positive observations (true positives) to all instances predicted as positive by the model, encompassing both correct and incorrect predictions (true positives and false positives). In the context of fault detection in a Zeta converter using a multi-class SVM:

- True Positives (TP): These are instances where the model correctly predicts a specific fault class among the Zeta converter faults.
- False Positives (FP): These are instances where the model incorrectly predicts a fault class when there is no fault or a different fault occurred in the Zeta converter.

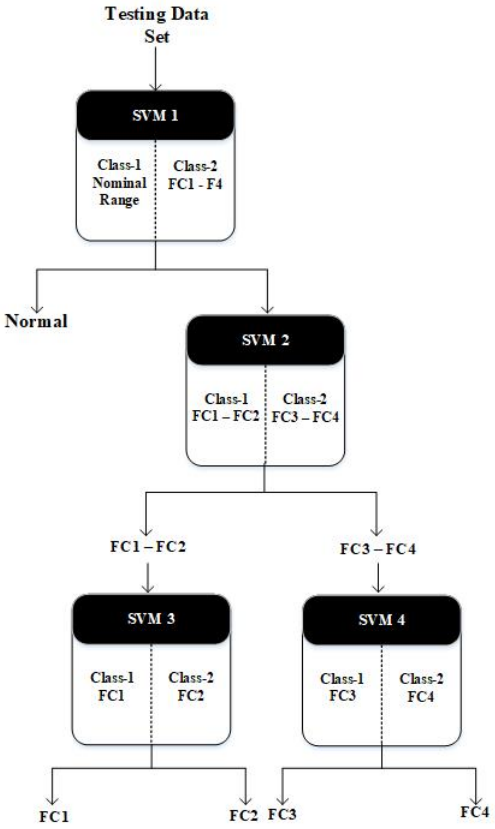

Fig. 10. Multi class SVM framework.

The precision score is calculated as:

$$precision = \frac{TP}{TP + FP} \tag{29}$$

A heightened precision value signifies that when the model predicts a fault class, it is more likely to be accurate. Precision gauges the model's accuracy in terms of minimizing false alarms, indicating that a higher precision corresponds to fewer false positives. This aspect is particularly crucial in situations where inaccurate fault predictions could result in unwarranted maintenance or intervention.

B. Recall

Recall, alternatively referred to as sensitivity or the true positive rate, is a performance metric employed to assess a classification model's capability to accurately identify all pertinent instances of a specific class or category within a dataset. The calculation for the recall score is:

$$Recall = \frac{TP}{TP + TN} \tag{30}$$

A heightened recall value signifies that the model excels in capturing all instances of a specific fault class. It evaluates the model's capacity to minimize the omission of positive instances or, in the context of fault detection, its effectiveness in identifying all instances of a particular fault in the Zeta converter.

C. F1 score

The F1 score serves as a unified metric that strikes a balance between precision and recall in classification tasks. It proves particularly valuable when taking into account both false positives and false negatives in the predictions made by my model.

- Precision is the proportion of correctly predicted positive observations out of all instances predicted as positive.
- Recall (or Sensitivity) is the proportion of correctly predicted positive observations out of all actual positive instances.

The F1 score is calculated as the harmonic mean of precision and recall. The formula for the F1 score is:

$$F1Score = \frac{2.precision.Recall}{precision + Recall} \tag{31}$$

The F1 score considers both false positives and false negatives and provides a balance between precision and recall. It helps to assess the overall accuracy of a classification model by considering both its ability to identify relevant instances (recall) and the proportion of correct positive predictions (precision). A high F1 score indicates both high precision and high recall, signifying a model that provides accurate positive predictions while capturing the most positive instances. In contrast, a low F1 score might indicate a model that either misses a lot of positive instances (low recall) or has many false positives (low precision).

D. Accuracy

Accuracy is a foundational performance metric employed to assess the overall correctness of a classification model. It quantifies the ratio of correctly predicted instances, encompassing both positive and negative, out of the total instances in the dataset.

- True Negatives (TN): Instances where the model correctly predicts the absence of a particular fault class in the Zeta converter.
- False Negatives (FN): Instances where the model incorrectly fails to predict a fault class when it is present.

The accuracy score is calculated as:

$$Accuracy = \frac{TP + TN}{TP + FN + FP + TN} \tag{32}$$

A higher accuracy value indicates that the model has made a higher proportion of correct predictions across all fault classes in the Zeta converter dataset.

E. Specificity

Specificity stands as a vital performance metric in classification tasks, especially in binary classification, to gauge a model's capability to accurately identify negative instances (true negatives) among all actual negative instances in a dataset. The calculation for specificity is:

$$Specificity = \frac{TN}{TN + FP} \tag{33}$$

A heightened specificity value signifies that the model excels in accurately identifying instances that are genuinely negative or instances that do not pertain to the considered class (such as the absence of faults in the context of fault detection). Specificity is especially beneficial in situations where the cost of false positives, i.e., incorrectly predicting a fault when none exists, is significant. In the case of fault detection in Zeta converters, accurately confirming the absence of certain faults is essential for ensuring the system's reliability. A high specificity implies a lower incidence of false alarms or erroneous identification of faults when they are not present, a critical aspect for maintaining the operational integrity of the Zeta converter. The analysis included the computation of these metrics for each sub-technique, relying on their respective confusion matrices. These metrics act as benchmarks to validate the models' performance in fault detection for the Zeta converter. This extensive evaluation framework aspired to offer a comprehensive insight into the strengths and limitations of each technique and sub-technique in fault detection, making a substantial contribution to the development of an effective fault detection system for Zeta converters. The classification process encompassed the application of diverse machine learning techniques and their corresponding sub-techniques, resulting in a thorough assessment of fault detection in the Zeta converter. These techniques comprised:

VII. Results

The SVM classification method was implemented using different kernel functions to explore distinct decision boundaries and their effectiveness in fault classification. The employed kernels encompassed linear, cubic, and quadratic functions, each offering a unique approach to delineating fault boundaries within the Zeta converter's operational data.

A. Linear SVM

A Linear SVM is a supervised machine learning algorithm used for classification tasks that work to create a linear decision boundary between different classes in a dataset. In the context of fault detection in a Zeta converter, the Linear SVM aims to separate various fault types using a straight line or hyperplane based on extracted features from the Zeta converter's operational data. It focuses on maximizing the margin (distance between the decision boundary and the nearest data points) to efficiently classify different fault instances. Table V presents the outcomes of the linear SVM as derived from the confusion matrices depicted in Fig. 11. Fig. 12 provides a graphical illustration demonstrating the efficacy of each evaluation metric in response to the results of each class.

B. Cubic SVM

A Cubic SVM is a variation of the SVM algorithm used for classification tasks, aiming to create a non-linear decision boundary between different classes within a dataset. In the context of fault detection in a zeta converter, the Cubic SVM extends the capabilities of the linear SVM by utilizing a cubic kernel function, allowing the model to capture more complex relationships between features. This cubic kernel transforms the input features into a higher-dimensional space, enabling the SVM to find nonlinear decision boundaries and classify Zeta converter fault instances that might not be linearly separable.

TABLE V. Results from Confusion Matric Linear SVM

Fault Classes	FC0	FC1	FC2	FC3	FC4	Average
precision	1	0.866	0.9066	0.866	0.858	0.8993
Recall	0.970	0.984	1	1	1	0.990
F1 Score	0.9847	0.921	0.951	0.928	0.9235	0.941
Accuracy	0.975	0.992	0.995	0.993	0.992	0.9897
Sensitivity	1	0.8666	0.9066	0.8666	0.8589	0.8997
Specificity	0.8778	0.999	1	1	1	0.9753

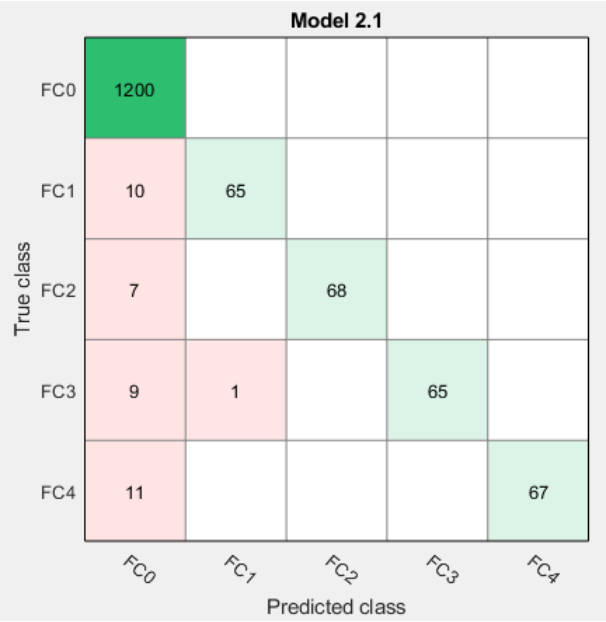

Fig. 11. Confusion matric linear SVM.

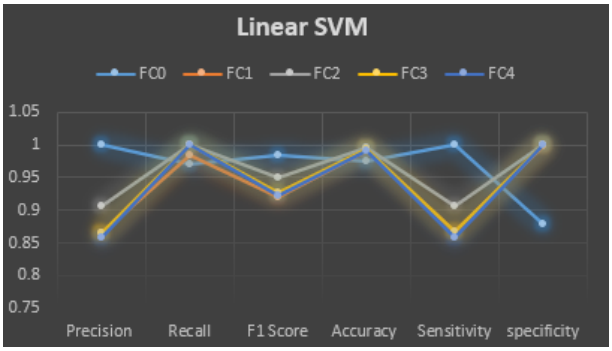

Fig. 12. Graphical representation of results from a confusion matrix for a linear SVM model.

TABLE VI. RESULTS FROM CONFUSION MATRIC CUBIC SVM

Fault Classes	FC0	FC1	FC2	FC3	FC4	Average
precision	1	0.906	0.920	0.866	0.923	0.9232
Recall	0.9787	0.985	0.971	1	1	0.9870
F1 Score	0.989	0.944	0.945	0.928	0.959	0.9531
Accuracy	0.9827	0.9946	0.995	0.993	0.9960	0.9922
Sensitivity	1	0.9066	0.92	0.8666	0.9230	0.9232
Specificity	0.9141	0.999	0.998	1	1	0.9822

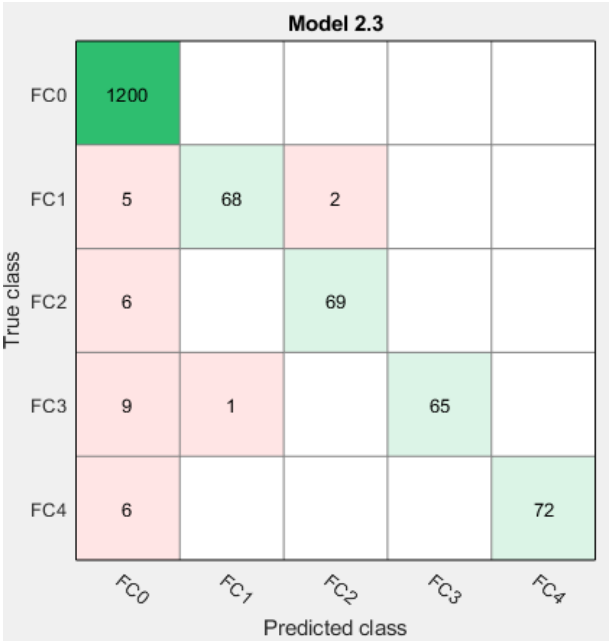

Fig. 13. Confusion matric cubic SVM.

Table VI presents the outcomes of the cubic SVM as derived from the confusion matrices depicted in Fig. 13. Fig. 14 provides a graphical illustration demonstrating the efficacy of each evaluation metric in response to the results of each class.

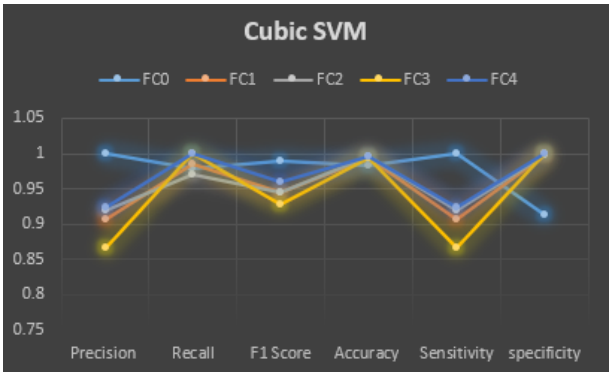

Fig. 14. Graphical representation of results from a confusion matrix for a cubic SVM model.

TABLE VII. RESULTS FROM CONFUSION MATRIC QUADRATIC SVM

Fault Classes	FC0	FC1	FC2	FC3	FC4	Average
precision	1	0.92	0.920	0.88	0.8846	0.9209
Recall	0.9756	1	1	1	1	0.9951
F1 Score	0.9876	0.9583	0.9583	0.9361	0.9387	0.9546
Accuracy	0.9800	0.9960	0.9960	0.9940	0.9940	0.992
Sensitivity	1	0.92	0.92	0.88	0.8846	0.9209
Specificity	0.9009	1	1	1	1	0.9801

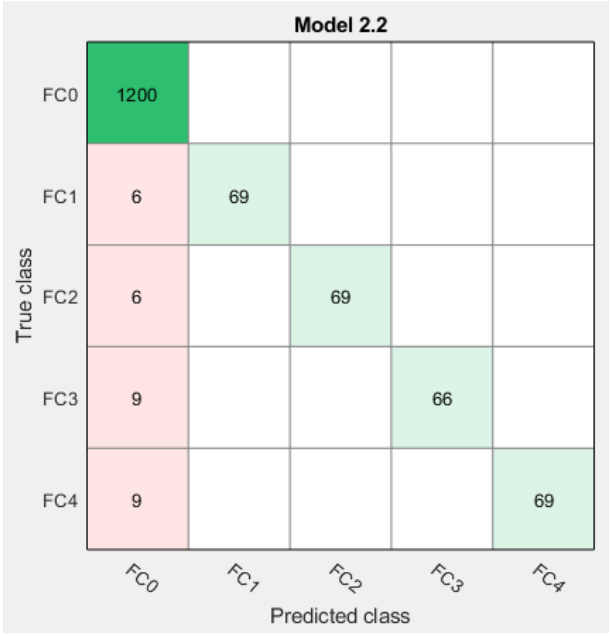

Fig. 15. Confusion matric quadratic SVM.

C. Quadratic SVM

A Quadratic SVM is a variant of the SVM algorithm used for classification tasks, specifically designed to create a non-linear decision boundary between different classes in a dataset. In the context of fault detection within a zeta converter, the Quadratic SVM extends the capabilities of linear SVM by employing a quadratic kernel function. This kernel allows the model to capture more complex relationships between features, transforming the input data into a higher-dimensional space where it can identify nonlinear patterns in the Zeta converter's operational data. Table VII presents the outcomes of the quadratic SVM as derived from the confusion matrices depicted in Fig. 15. Fig. 16 provides a graphical illustration demonstrating the efficacy of each evaluation metric in response to the results of each class.

VIII. KNN

Utilized the KNN algorithm, and multiple distance metrics were applied to evaluate the proximity of data points within the feature space. The variations in distance metrics, including fine, cubic, cosine, and coarse distances, provided a comprehensive analysis of different neighborhood structures and their influence on fault classification accuracy.

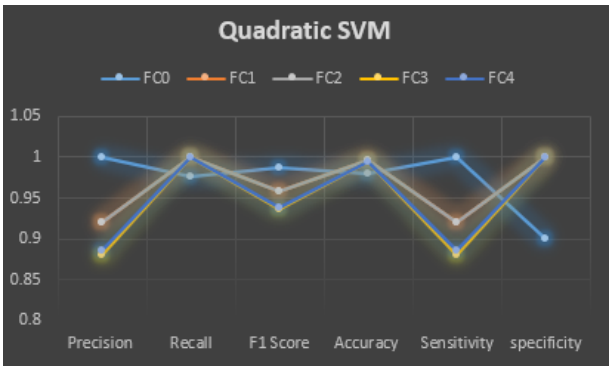

Fig. 16. Graphical representation of results from a confusion matrix for a quadratic SVM model.

TABLE VIII. RESULTS FROM CONFUSION MATRIC FINE KNN

Fault Classes	FC0	FC1	FC2	FC3	FC4	Average
precision	0.9842	0.9480	0.9594	0.8933	0.9473	0.9464
Recall	0.8069	0.0487	0.0475	0.0449	0.04828	0.1992
F1 Score	0.8867	0.0926	0.0905	0.0855	0.0918	0.2494
Accuracy	0.9787	0.9927	0.9953	0.9926	0.9933	0.9905
Sensitivity	0.9891	0.9733	0.9466	0.9571	0.9230	0.9578
Specificity	0.9372	0.9971	0.9978	0.9944	0.9971	0.9755

A. Fine KNN

A fine KNN is a variant of the KNN algorithm used for classification tasks, focusing on a finer level of granularity in assessing neighboring data points. In the context of fault detection in a zeta converter, the fine KNN algorithm involves considering a smaller number of nearest neighbors within the feature space. This approach aims to make more precise distinctions between different fault classes based on the characteristics of the zeta converter's operational data. Table VIII presents the outcomes of the fine KNN as derived from the confusion matrices depicted in Fig. 17. Fig. 18 provides a graphical illustration demonstrating the efficacy of each evaluation metric in response to the results of each class.

B. Cubic KNN

A Cubic KNN is a variation of the KNN algorithm used for classification tasks, aiming to consider a larger and more expanded neighborhood of neighboring data points within the feature space. Table IX presents the outcomes of the cubic KNN as derived from the confusion matrices depicted in Fig. 19. Fig. 20 provides a graphical illustration demonstrating the efficacy of each evaluation metric in response to the results of each class.

C. Cosine KNN

Cosine KNN is a variant of the KNN algorithm that leverages the cosine similarity metric to determine the proximity of data points within the feature space. In the context of fault detection in a zeta converter, cosine KNN measures the angle between data points in a multi-dimensional space rather than

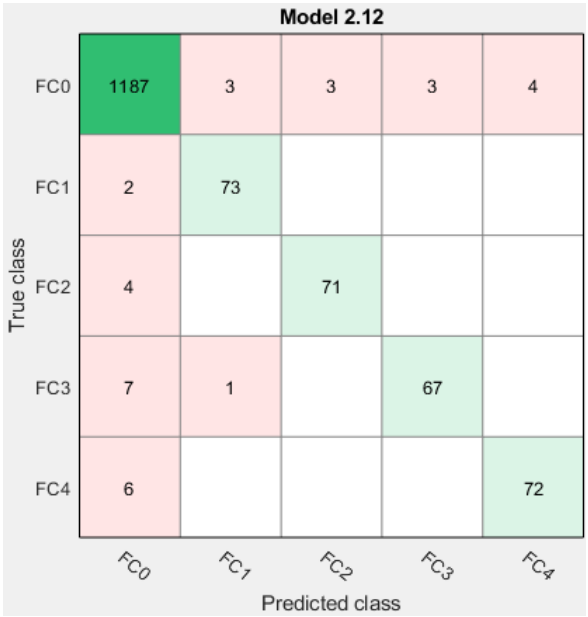

Fig. 17. Confusion matric fine KNN.

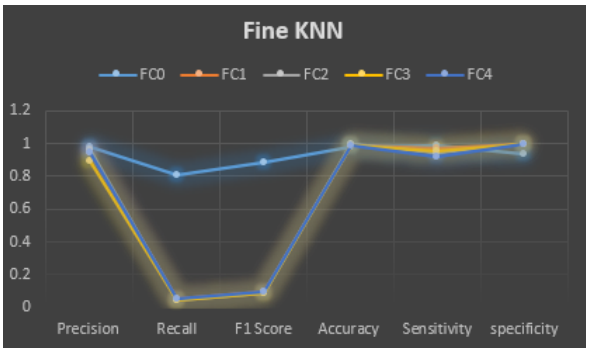

Fig. 18. Graphical representation of results from a confusion matrix for a fine KNN model.

TABLE IX. RESULTS FROM CONFUSION MATRIC CUBIC KNN

Fault Classes	FC0	FC1	FC2	FC3	FC4	Average
precision	0.9672	0.9843	0.9714	1	1	0.9845
Recall	0.8202	0.0422	0.0458	0.0435	0.0429	0.1989
F1 Score	0.8876	0.0809	0.0874	0.0833	0.0822	0.2442
Accuracy	0.9733	0.9913	0.9940	0.9933	0.9906	0.9885
Sensitivity	1	0.84	0.9066	0.8666	0.8205	0.8867
Specificity	0.8674	0.9992	0.9985	1	1	0.9730

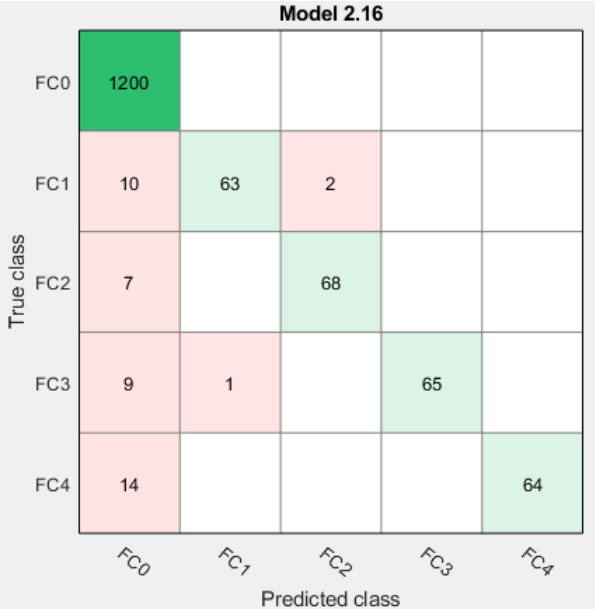

Fig. 19. Confusion matric cubic KNN.

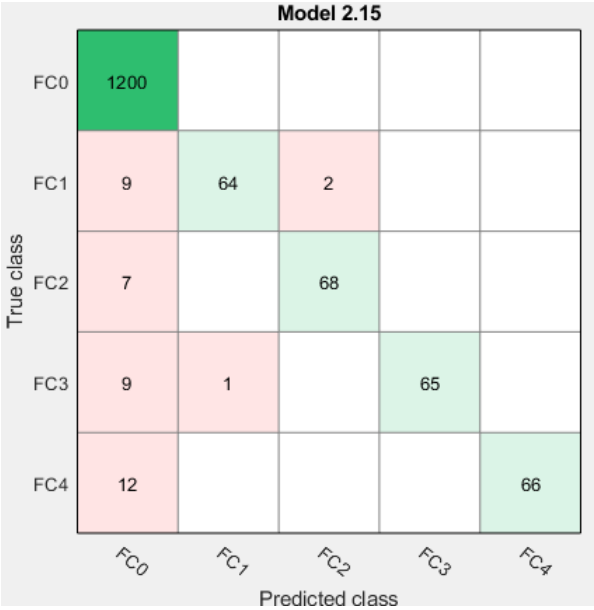

Fig. 21. Confusion matric cosine KNN.

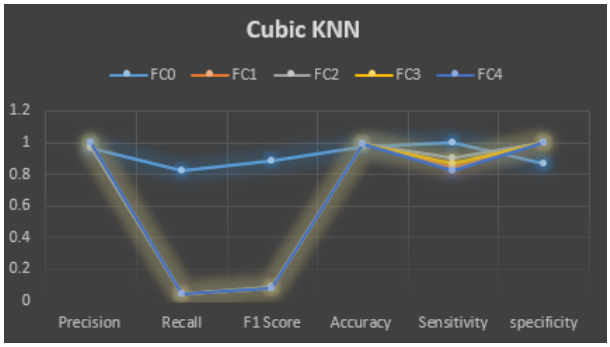

Fig. 20. Graphical representation of results from a confusion matrix for a cubic KNN model.

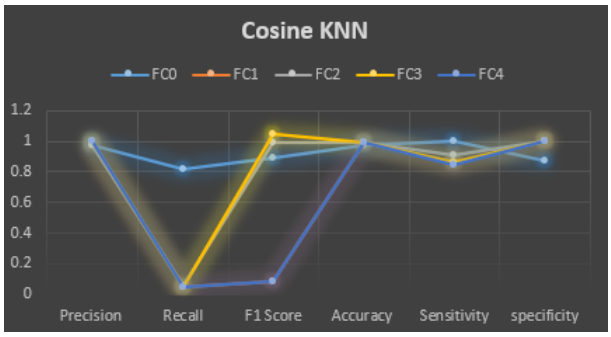

Fig. 22. Graphical representation of results from a confusion matrix for a cosine KNN model.

the direct Euclidean distance. Table X presents the outcomes of the cosine KNN as derived from the confusion matrices depicted in Fig. 21. Fig. 22 provides a graphical illustration demonstrating the efficacy of each evaluation metric in response to the results of each class.

TABLE X. RESULTS FROM CONFUSION MATRIC COSINE KNN

Fault Classes	FC0	FC1	FC2	FC3	FC4	Average
precision	0.970	0.984	0.971	1	1	0.985
Recall	0.8185	0.0429	0.0525	0.0502	0.0442	0.2012
F1 Score	0.8877	0.0821	0.0995	1.0478	0.0846	0.4394
Accuracy	0.9753	0.9920	0.9930	0.9940	0.9920	0.9892
Sensitivity	1	0.8533	0.9066	0.8666	0.8461	0.8945
Specificity	0.8728	0.999	0.9983	1	1	0.9740

D. Coarse KNN

The Coarse KNN is a variant of the KNN algorithm used for classification tasks, where it considers a broader and more generalized neighborhood of data points within the feature space. In the context of fault detection in a zeta converter, the coarse KNN algorithm involves examining a larger set of neighboring data points to provide a more generalized analysis of the zeta converter's operational data. Table XI presents the outcomes of the coarse KNN as derived from the confusion matrices depicted in Fig. 23. Fig. 24 provides a graphical illustration demonstrating the efficacy of each evaluation metric in response to the results of each class.

IX. DECISION TREE

The Decision Tree methodology was implemented with varying tree complexities to discern the hierarchy of fault features. Different tree complexities fine tree, medium tree, and coarse tree were employed to study the trade-off between model simplicity and the ability to capture intricate fault patterns in the zeta converter's operation.

TABLE XI. RESULTS FROM CONFUSION MATRIC COARSE KNN

Fault Classes	FC0	FC1	FC2	FC3	FC4	Average
precision	0.8426	0.9615	1	1	1	0.9608
Recall	0.9382	0.0172	0.0076	0.0151	0.0138	0.1983
F1 Score	0.8878	0.0337	0.0150	0.0297	0.0272	0.1986
Accuracy	0.8509	0.9667	0.9574	0.9647	0.9614	0.9402
Sensitivity	1	0.333	0.1466	0.2933	0.2564	0.4058
Specificity	0.2607	0.999	1	1	1	0.8519

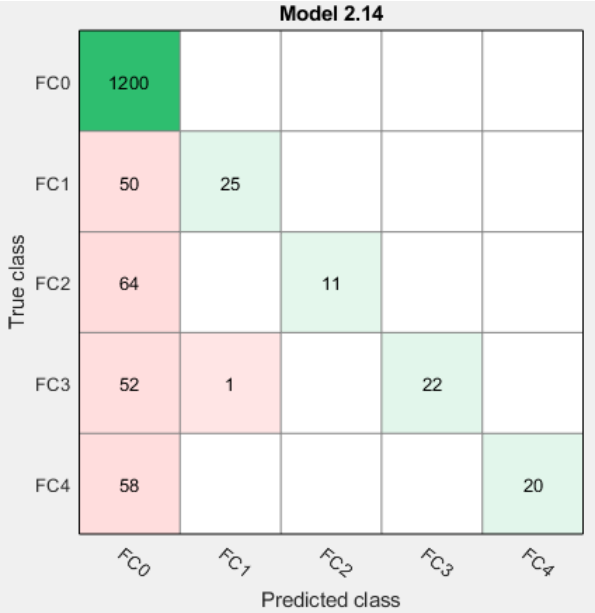

Fig. 23. Confusion matric coarse KNN.

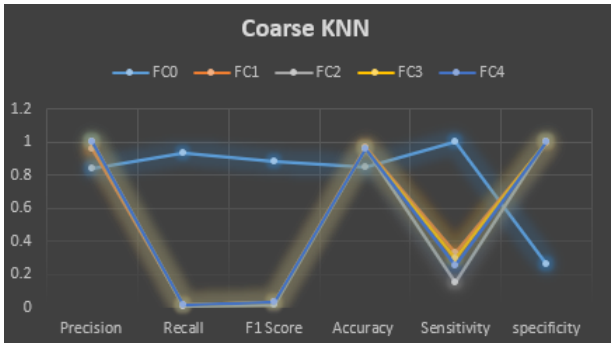

Fig. 24. Graphical representation of results from a confusion matrix for a coarse KNN model.

TABLE XII. RESULTS FROM CONFUSION MATRIC FINE TREE

Fault Classes	FC0	FC1	FC2	FC3	FC4	Average
precision	0.9916	1	0.9729	0.9605	0.9615	0.9782
Recall	0.8024	0.0486	0.0480	0.0487	0.0499	0.1995
F1 Score	0.8870	0.0926	0.0915	0.0926	0.0948	0.2517
Accuracy	0.9866	0.9986	0.9966	0.9966	0.9960	0.9948
Sensitivity	0.9916	0.9733	0.96	0.9733	0.9615	0.9719
Specificity	0.9669	1	0.9985	0.9978	0.9979	0.9922

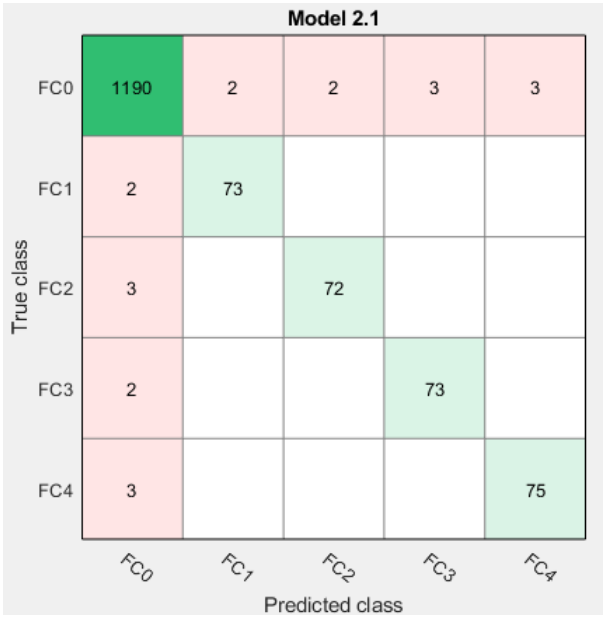

Fig. 25. Confusion matric fine tree.

A. Fine Tree

A Fine Tree is a classification model that employs a decision tree algorithm with a more detailed or intricate structure. In the context of fault detection in a zeta converter, a fine decision tree aims to create a tree structure with more levels, nodes, or branches, allowing for a more intricate analysis of features related to different fault classes. Table XII presents the outcomes of the fine Tree as derived from the confusion matrices depicted in Fig. 25. Fig. 26 provides a graphical illustration demonstrating the efficacy of each evaluation metric in response to the results of each class.

B. Medium Tree

A Medium Tree is a classification model that utilizes a decision tree algorithm with a moderate level of complexity. In the context of fault detection in a zeta converter, a medium decision tree involves creating a tree structure with a moderate number of levels, nodes, or branches. This balanced complexity allows for a middle-ground analysis of features related to different fault classes. Table XIII presents the outcomes of the medium tree as derived from the confusion matrices depicted in Fig. 27. Fig. 28 provides a graphical illustration demonstrating the efficacy of each evaluation metric in response to the results of each class.

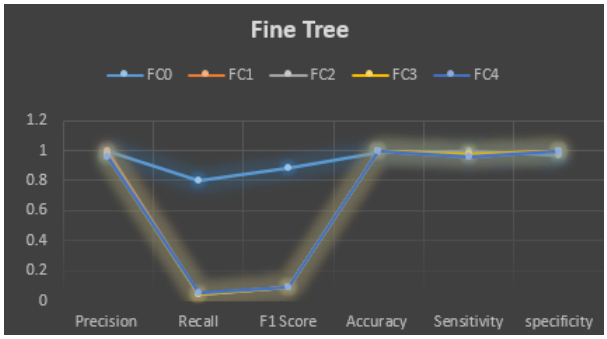

Fig. 26. Graphical representation of results from a confusion matrix for a fine tree model.

TABLE XIII. RESULTS FROM CONFUSION MATRIC MEDIUM TREE

Fault Classes	FC0	FC1	FC2	FC3	FC4	Average
precision	0.9916	0.9733	0.9729	0.9605	0.9615	0.9719
Recall	0.8024	0.0486	0.0480	0.0486	0.0501	0.1995
F1 Score	0.8870	0.0925	0.0914	0.0925	1.9504	0.6227
Accuracy	0.9866	0.9973	0.9966	0.9966	0.9960	0.9945
Sensitivity	0.9916	0.9732	0.9729	0.9605	0.9615	0.9719
Specificity	0.9916	0.9733	0.5675	0.9605	0.9615	0.8908

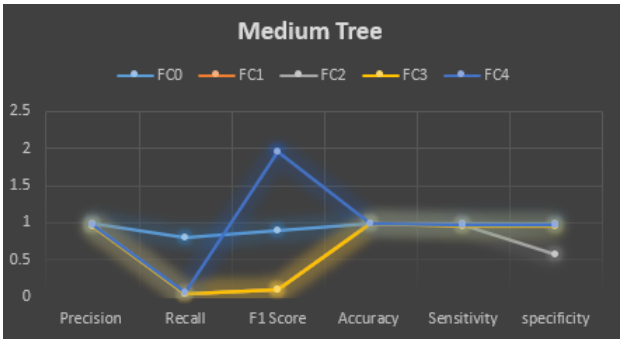

Fig. 27. Confusion matric medium tree.

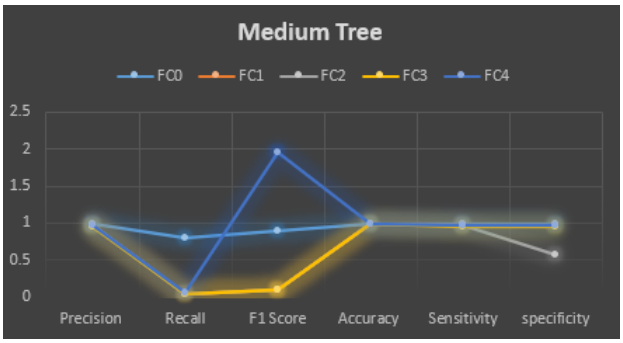

Fig. 28. Graphical representation of results from a confusion matrix for a medium tree model.

TABLE XIV. RESULTS FROM CONFUSION MATRIC COARSE TREE

Fault Classes	FC0	FC1	FC2	FC3	FC4	Average
precision	0.9558	1	0.9729	0.9361	0.9615	0.9652
Recall	0.8275	0.0383	0.0480	0.0299	0.0501	0.1987
F1 Score	0.8870	0.0737	0.0914	0.0579	0.0952	0.2410
Accuracy	0.9580	0.9880	0.9966	0.9773	0.9960	0.9831
Sensitivity	0.9933	0.76	0.96	0.5866	0.9615	0.8522
Specificity	0.8184	1	0.9985	0.9978	0.9978	0.9625

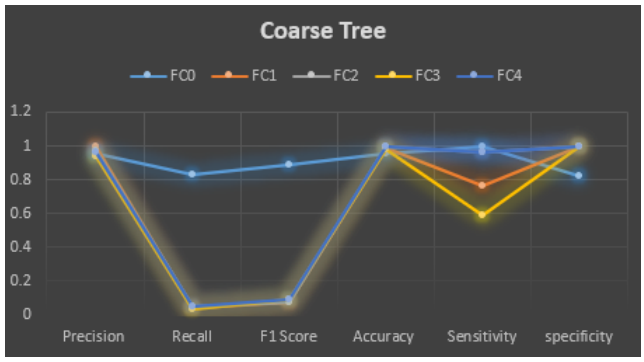

Fig. 29. Confusion matric coarses tree.

C. Coarse Tree

A Coarse Tree is a classification model that employs a decision tree algorithm with a simpler or more generalized structure. In the context of fault detection in a zeta converter, a Coarse decision tree aims to create a tree structure with fewer levels, nodes, or branches, facilitating a more generalized analysis of features related to different fault classes. Table XIV presents the outcomes of the coarse tree as derived from the confusion matrices depicted in Fig. 29. Fig. 30 provides a graphical illustration demonstrating the efficacy of each evaluation metric in response to the results of each class.

X. DISCUSSION

The research demonstrates the viability of SVMs for monitoring Zeta converters. The chosen quadratic SVM achieved

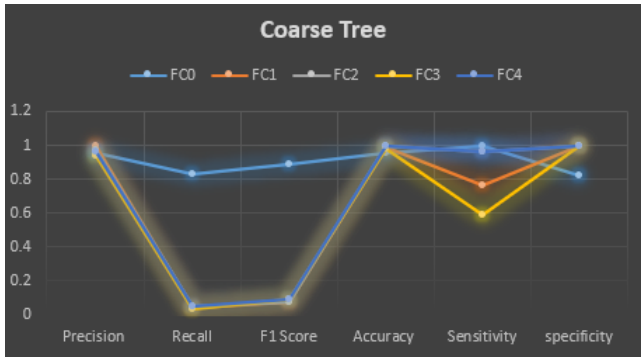

Fig. 30. Graphical representation of results from a confusion matrix for a coarse tree model.

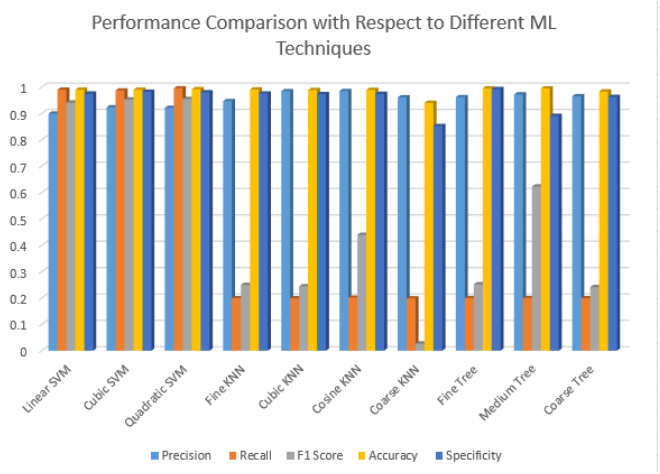

Fig. 31. Graphical representation of performance comparison across various machine learning techniques.

promising results in identifying converter health based on the collected passive element data.This suggests that analyzing these readily available measurements holds promise for preventative maintenance and fault detection in smart grids. While various SVM algorithms were explored, the quadratic SVM emerged as the most effective in this specific application. This could be attributed to the underlying non-linear relationships between the passive element data and converter health. The quadratic SVM's ability to learn and exploit these non-linear relationships likely contributed to its superior performance. This research acknowledges certain limitations. Firstly, the study utilized a simulated dataset or a controlled experimental setup. Real-world data from deployed converters might introduce additional complexities and noise that could impact model performance. Secondly, the chosen features (passive element current and voltage) might not be the most comprehensive. Exploring additional features or feature engineering techniques could potentially improve the model's accuracy. The goal is to In Fig. 31, provide a comprehensive overview of how these techniques fare concerning criteria such as accuracy, precision, recall, ,F1 score and Specificity among others, and quadratic SVM yields superior results compared to other machine learning techniques employed in training our dataset. quadratic SVMs can handle various data types as long as they are numerically represented. The key factor for successful application is whether the data can be effectively separated (linearly or using kernels) in the high-dimensional space for classification. Building on this work, future research could explore the following avenues:

1) Real-world data integration: Test the model's effectiveness with data collected from actual Zeta converters deployed in smart grid environments.
2) One-against-one (OvO)Feature engineering and optimization: Investigate the incorporation of additional data points or the optimization of existing features to enhance the model's discriminatory power.
3) Hybrid model development: Explore the potential of combining SVMs with other machine learning algorithms, such as deep learning architectures, for more robust and comprehensive converter health monitoring.

XI. Conclusion

In this paper, we embarked on a journey to explore the intricate relationship between renewable energy variations and their impact on the passive components of Zeta converters. Utilizing MATLAB Simulink for simulation, we meticulously gathered and analyzed data on the currents and voltages across these components under varying renewable energy conditions. Our objective was to deeply understand how fluctuations in renewable energy sources affect the operation and stability of Zeta converters. To achieve this, we employed a sophisticated machine learning approach, leveraging a multi-class SVM classifier. This method proved instrumental in distinguishing between nominal and malfunctioning conditions of the Zeta converter with remarkable accuracy. We compared several machine learning techniques, including SVM with different kernel functions (linear, cubic, and quadratic), KNN with a range of distance metrics (fine, cubic, cosine, coarse), and Decision Trees with varying complexities (fine, medium, coarse). Among these, the linear SVM emerged as the standout performer, delivering superior results in terms of accuracy, sensitivity, specificity, precision, recall, and F1 score. Additionally, the SVM's computational efficiency, especially when using RBF and polynomial kernels, highlighted its practicality for real-world applications. One of the pivotal challenges encountered in training the classification learner was the algorithm's performance variability across different scenarios, such as changes in the size of training data and solar operating conditions. Despite these challenges, the multi-class SVM consistently demonstrated optimal performance, accurately predicting component conditions under a wide range of operational scenarios. This included both gradual degradation and critical failure conditions, affirming its robustness and reliability as a diagnostic tool. Moreover, the SVM's unparalleled accuracy in forecasting component health under varied operational states, including during the degradation phase, underscores its potential for real-time monitoring and preventive maintenance of Zeta converters. This capability is particularly valuable in ensuring the longevity and efficiency of systems integrated with renewable energy sources, where operational conditions are inherently dynamic and unpredictable. Thus, this research not only sheds light on the dynamic effects of renewable energy variations on Zeta converters but also establishes the multi-class SVM as a powerful tool for predictive maintenance and fault diagnosis in smart grid applications. The insights gained from this study pave the way for further exploration into machine learning-based solutions for enhancing the reliability and sustainability of renewable energy systems.

References

[1] H. Sharma et al. "Feasibility of Solar Grid-Based Industrial Virtual Power Plant for Optimal Energy Scheduling: A Case of Indian Power Sector", *Energies*, 2022 doi.org/10.3390/en15030752.

[2] F. Azeem et al. "Load Management and Optimal Sizing of Special-Purpose Microgrids Using Two Stage PSO-Fuzzy Based Hybrid Approach", *Energies*, 2022 doi.org/10.3390/en15176465.

[3] Asif, Rao Muhammad, et al. "Design and analysis of robust fuzzy logic maximum power point tracking based isolated photovoltaic energy system." Engineering Reports 2.9 (2020): e12234.

[4] N. Vasudevan et al. "Design and Development of an Intelligent Energy Management System for a Smart Grid to Enhance the Power Quality, *Energy Engineering* 120, 1747-176, 2023

[5] Zhang, Chaolong, et al. "A novel approach for analog circuit fault prognostics based on improved RVM." Journal of Electronic Testing 30 (2014): 343-356.

[6] Luchetta, Antonio, et al. "MLMVNNN for parameter fault detection in PWM DC–DC converters and its applications for buck and boost DC–DC converters." IEEE Transactions on Instrumentation and Measurement 68.2 (2018): 439-449.

[7] Ko, Y-J., et al. "Fault diagnosis of three-parallel voltage-source converter for a high-power wind turbine." IET Power Electronics 5.7 (2012): 1058-1067.

[8] Wang, Li, et al. "A novel remaining useful life prediction approach for superbuck converter circuits based on modified grey wolf optimizer-support vector regression." Energies 10.4 (2017): 459.

[9] Markovic, Nikola, et al. "Condition monitoring for power converters via deep one-class classification." 2021 20th IEEE International Conference on Machine Learning and Applications (ICMLA). IEEE, 2021.

[10] Kaplan, Halid, Kambiz Tehrani, and Mo Jamshidi. "A fault diagnosis design based on deep learning approach for electric vehicle applications." Energies 14.20 (2021): 6599.

[11] Zhao, Shuai, et al. "Parameter estimation of power electronic converters with physics-informed machine learning." IEEE Transactions on Power Electronics 37.10 (2022): 11567-11578.

[12] Alam, Mohammed Khorshed, and Faisal H. Khan. "Reliability analysis and performance degradation of a Boost converter." 2013 IEEE Energy Conversion Congress and Exposition. IEEE, 2013.

[13] Kulkarni, C., Gautam Biswas, and Xenofon Koutsoukos. "A prognosis case study for electrolytic capacitor degradation in DC-DC converters." PHM Conference. 2009.

[14] H. Maqbool et al. "An Optimized Fuzzy Based Control Solution for Frequency Oscillation Reduction in Electric Grids", *Energies*, 2022, doi.org/10.3390/en15196981.

[15] S Balouch et al. "Optimal Scheduling of Demand Side Load Management of Smart Grid Considering Energy Efficiency", *Energy Res.*, 2022, doi.org/10.3389/fenrg.2022.861571

[16] M. Asif et al. "Industrial Automation Information Analogy for Smart Grid Security", *CMC-Computers, Materials & Continua* 71, 3985-3999, 2022, doi:10.32604/cmc.2022.023010

[17] M.L. Katche, Musong L. et al. "A Comprehensive Review of Maximum Power Point Tracking (MPPT) Techniques Used in Solar PV Systems" *Energies*, 2023, doi.org/10.3390/en16052206

[18] A. Yousaf et al. "An improved residential electricity load forecasting using a machine-learning-based feature selection approach and a proposed integration strategy." Sustainability 13.11 (2021): 6199.

[19] K. Mahmoud, and M. Lehtonen, "Comprehensive analytical expressions for assessing and maximizing technical benefits of photovoltaics to distribution systems." IEEE Transactions on Smart Grid 12.6 (2021): 4938-4949.

[20] K. Rahbar, J. Xu, and R. Zhang. "Real-time energy storage management for renewable integration in microgrid: An off-line optimization approach." IEEE Transactions on Smart Grid 6.1 (2014): 124-134.

[21] W. Wang et al. "Energy management and optimization of vehicle-to-grid systems for wind power integration." CSEE Journal of Power and Energy Systems 7.1 (2020): 172-180.

[22] Yousaf, Adnan, et al. "A novel machine learning-based price forecasting for energy management systems." Sustainability 13.22 (2021): 12693.

[23] A. Waqar, et al. "Machine learning based energy management model for smart grid and renewable energy districts." IEEE Access 8 (2020): 185059-185078.

[24] Siddique, Muhammad Abu Bakar, et al. "Maximum power point tracking with modified incremental conductance technique in grid-connected PV array." 2020 5th International Conference on Innovative Technologies in Intelligent Systems and Industrial Applications (CITISIA). IEEE, 2020.

[25] M. Bindi et al. "Comparison between pi and neural network controller for dual active bridge converter." 2021 IEEE 15th International Conference on Compatibility, Power Electronics and Power Engineering (CPE-POWERENG). IEEE, 2021.

[26] Jørgensen, Asger Bjørn. "Derivation, Design and Simulation of the Zeta converter." (2021).

[27] Divyasharon, R., R. Narmatha Banu, and D. Devaraj. "Artificial neural network based MPPT with CUK converter topology for PV systems under varying climatic conditions." 2019 IEEE International Conference on Intelligent Techniques in Control, Optimization and Signal Processing (INCOS). IEEE, 2019.

[28] Ni, Yuanping, and Junli Li. "Faults diagnosis for power transformer based on support vector machine." 2010 3rd International Conference on Biomedical Engineering and Informatics. Vol. 6. IEEE, 2010.

[29] M. Galar et al. "An overview of ensemble methods for binary classifiers in multi-class problems: Experimental study on one-vs-one and one-vs-all schemes." Pattern Recognition 44.8 (2011): 1761-1776.

[30] Widodo, Achmad, and Bo-Suk Yang. "Support vector machine in machine condition monitoring and fault diagnosis." Mechanical systems and signal processing 21.6 (2007): 2560-2574.